PNAS
www.pnas.org

Supporting Information for

Regulation of Acetate Metabolism : Coordination with the TCA cycle via a Processed Small RNA.

François De Mets, Laurence Van Melderen, and Susan Gottesman[*]

Susan Gottesman
Email: gottesms@mail.nih.gov

This PDF file includes:

Supplementary Materials and Methods
Figs. S1 to S9
Tables S1 to S3
References for SI reference citations

www.pnas.org/cgi/doi/10.1073/pnas.1815288115

Supporting Information

SI Materials and Methods

Bacterial strain construction

The *ackA-lacZ* (FDM1700), *ackA*-lacZ* (FDM1706) and *pta-lacZ* (FDM1705) translational fusion reporter strains were generated by phage λ Red-mediated recombineering in PM1805; recombinants were selected on M63 minimal sucrose agar as previously described (1, 2). The first ten codons of *ackA* or the first nine codons of *pta* as well as the entire leader sequence of each gene were amplified by PCR from MG1655 template genomic DNA and fused to *lacZ* regulated by an arabinose-inducible P_{BAD} promoter, by using primers FDM1/FDM2, FDM1/FDM3, FDM4/FDM5, respectively. The *ackA* and *pta* translational fusions were constructed with a 5′ leader of 223 (for *ackA*) and 263 (for *pta*) nucleotides based on TSS mapping using differential RNA sequencing data in *E. coli* (3). λ Red-mediated recombineering in NM580, which contains *kan*-pBAD-*ccdB* upstream of *lacZ* at the chromosomal *lacI-lacZ* site, was used as the background strain to generate *pta-lacZ* transcriptional fusion reporter strains (strains FDM1719, FDM1720, FDM1721, FDM1722, FDM1723, FDM1724). A gBlock gene fragment (FDM20) was used to generate FDM1719 while a PCR fragment was generated for FDM1720, 1721, 1722, 1723 and 1724 with primers FDM22/FDM21, FDM23/FDM21, FDM24/FDM21, FDM25/FDM21, FDM25/26 respectively. Recombinants were selected on LB+arabinose 0.2% plates (CcdB toxin induction) and screened for their sensitivity to kanamycin. FDM1719 was used as a control strain for the experiment with *pta-lacZ* transcriptional fusion reporter strains. The sRNA plasmid library was expressed from an IPTG-inducible pBRplac plasmid, as previously described (4). SdhX* and SdhX** were generated using the Quickchange II site-directed mutagenesis kit (Stratagene) with primers FDM12/FDM13 and FDM27/FDM28 following the manufacturer's instructions. The chromosomal FDM1712 *ackA** mutant was constructed by a two-step procedure. First, P1 transduction from FDM1609 was used to create an *ackA::kan*$^{R\text{-}KEIO}$ derivative of a strain containing the mini-λ for recombineering. This *ackA* null strain is unable to grow anaerobically on xylose. After λ Red-mediated recombineering with a PCR fragment using primers FDM15/FDM16, recombinants were selected in anaerobic conditions on MOPS+xylose 0.2% plates to yield FDM1712. To construct the chromosomal FDM1614 and FDM1716 Pta-FLAG-*zeo* strain (where FLAG is the epitope tag and Zeo the zeocin resistance protein), a gBlock fragment FDM14 comprising 3XFLAG-*zeo* was introduced by λ Red recombineering in WT NM541 and FDM1712 strains, respectively. The chromosomal FDM1652 SdhX^{seedless} and its WT derivative FDM1653 were constructed by λ Red recombineering in the NM580 background using gBlock fragments FDM108 and FDM109, respectively. All the chromosomal modifications or derivatives of parent strains were verified by Sanger sequencing and transduced to a fresh genetic background using bacteriophage P1*vir* as described by Miller (5), then checked by PCR. Phage λ Red-mediated recombineering was used to construct deletion alleles marked by Kan^R flanked by FRT (FLP Recognition Target) sites, which were amplified from the *tolC* ::kan$^{R\text{-}KEIO}$ allele in ASP6028 (6-8). Deletion alleles marked by Zeo^R were amplified from NM580. When multiple alleles were deleted, the resistance cassette was removed by introduction of the FLP expression plasmid pCP20 (9) for each insert before introducing the next allele.

RNA extraction and Northern Blot analysis

In the case of mRNA Northern blots, 10 µg of total RNA was loaded on an agarose gel (1.2% in MOPS buffer). In the case of sRNA Northern blots, 5 µg of total RNA was loaded on a 6% or 10% Novex™ TBE-Urea Gel (ThermoFisher). RNA were transferred to a Zeta-Probe GT blotting membrane (Bio-Rad) overnight by capillarity (agarose gel) or for 2 hours at 200 mA by electro-transfer (TBE-Urea gel). Membranes were then UV cross-linked and hybridized overnight at 42ºC with the biotinylated probe(s) (SI Appendix, Table S3) in ULTRAhyb Hybridization Buffer (ThermoFisher), then further incubated with a streptavidin-conjugated alkaline phosphatase. The blot was developed using the BrightStar BioDetect kit (Thermofisher) according to the manufacturer's instructions. The chemifluorescence was captured using the ChemiDoc™ MP Imaging System (Bio-Rad) and quantification was performed using the Image Studio software (Li-COR Biosciences). Even in cases where signals appeared to be low (for instance, SdhX in LB-grown cultures in SI Appendix, Fig. S6C), the measurement of signal by the imaging system showed a 800x better signal than background even for the band with the lowest value. *ackA*, *pta* and SsrA were respectively detected using probes FDM37, 38 and 39. SdhX was detected using probe FDM41 (except in SI Appendix, Fig. S5A, in which probe FDM40 was used), ArcZ with FDM42, rRNA 5S with FDM43 and *sdhC* with FDM44.

5′ RACE

Detection of *pta* mRNA 5′ ends were performed by 5′ Rapid Amplification of cDNA Ends (RACE) as previously described (1) with minor modifications. RNA was extracted from WT strain NM525, grown in LB to an OD_{600} of 0.5. Samples were treated with Baseline-ZERO DNase (Epicentre Technologies, 25U) to remove any traces of genomic DNA. RNA extracts were then treated with Tobacco Acid Pyrophosphatase (TAP, Epicentre Technologies) to convert RNA 5′ triphosphates to 5′ monophosphates. Control RNA was incubated in the absence of TAP. An RNA adapter (FDM30) was then ligated to RNA with 40U of T4 RNA ligase 1 (New Englands Biolabs). Adapter-ligated RNAs were reverse transcribed using 200U of SuperScript IV RT (Invitrogen) according to the manufacturer's instructions, followed by RNase H treatment (New England Biolabs, 1U). cDNAs were then amplified by PCR using the adapter-specific primer FDM32 and a gene-specific primer FDM31. The PCR product was then TOPO cloned into the pCR4-TOPO vector (Invitrogen) and transformants were analyzed and sequenced as previously described (10).

TDE digestion

Total RNA (5µg) isolated with the hot acid phenol procedure from MG1655 WT cells grown to OD_{600} of 1 in LB was either left untreated (-) or incubated with 5′ monophosphate-dependent terminator exonuclease (TDE) (+) (Epicentre) as described previously (11) and run on a 6% Novex™ TBE-Urea gel (Thermo Fisher Scientific). The membrane was probed for the SdhX-specific and ArcZ-specific biotinylated probes; ArcZ has been previously shown to be processed from a full-length transcript (ArcZ) to an abundant shorter form (ArcZ-S) and serves as a control.

In vitro RNA structure probing

About 0.3 pmol of 5′ end ^{32}P-radiolabeled $SdhX_{101}$ sRNA was denaturated for 1 min at 95°C. After cooling down on ice for 5 min, the RNA was mixed with 1µg of yeast RNA and 10× structure buffer, then incubated for 10 min at room temperature. Samples were either treated for 2 or 4 min with 2µl of 25 mM of fresh lead(II) acetate solution (Fluka) or 4 or 6 min with 2µl of 0.01U/µl RNase T1 (Ambion). Alkaline and RNase T1 ladders were

generated by either incubating 0.3 pmol of denaturated RNA for 5 min at 95°C in the alkaline hydrolysis buffer (Ambion) or with 0.1U RNase T1 for 5 min at 37°C in 1× sequencing buffer (Ambion). Reactions were stopped with 10µl of loading buffer II (Ambion). After denaturation for 5 min at 95°C, samples were resolved on an 8% polyacrylamide urea sequencing gel in 1× TBE at 70W for 80 min. Gel was vacuum-dried for 1h at 80°C and exposed overnight to a phosphorimager.

Western Blotting

Endogenous AckA was detected using rabbit polyclonal anti-AckA from Abcam and Pta-FLAG was detected using mouse monoclonal anti-FLAG® M2 (Sigma-Aldrich). To examine the effect of SdhX, cell cultures were diluted 500-fold from overnight cultures in fresh medium, including IPTG and ampicillin for strains carrying plasmids. 1 ml of bacterial cultures were collected as indicated. After TCA precipitation and acetone neutralization, pellets were suspended in 1X SDS Blue Loading Buffer (New England Biolabs) and boiled at 95 °C for 10 min to lyse the cells. For all experiments, equal amounts of total protein samples were loaded and separated on a 4-12% Bis-Tris polyacrylamide NuPAGE gel (Invitrogen) in 1X MOPS SDS running buffer (Invitrogen). Protein samples were transferred to a nitrocellulose membrane using an iBlot2 gel transfer device (Invitrogen). The membrane was blocked for 30min in PBS with 5% nonfat dry milk and then incubated with negatively adsorbed rabbit polyclonal anti-AckA (Abcam; 1:500) or mouse monoclonal anti-FLAG® M2 (Sigma-Aldrich; 1:1000) antibodies in PBST with 5% nonfat dry milk for 1h at room temperature. Blots were washed three times with PBST, followed by another hour incubation step with Goat anti-rabbit IgG StarBright™ Blue 700 (Bio-Rad, 1:5000) and Goat anti-mouse IgG DyLight®800 (Bio-Rad, 1:10000) and PBST washes. Fluorescence signals were captured using the imaging system ChemiDoc MP (Bio-Rad) and quantified with the Image Studio software (Li-COR Biosciences).

Acetyl-phosphate measurements

Aliquots of cell cultures in mid-exponential phase (OD_{600} 0.4-0.5) were centrifuged at 4,000 x g for 10 min at 4°C. Cell pellets were suspended in ice-cold assay buffer (10 mM sodium phosphate pH 7.5, 10 mM $MgCl_2$, 1mM EDTA) using 500 µl per OD_{600} of cells. Total protein content was determined by mixing 50 µl of each sample with SDS 1% and heated at 95°C for 5 min. Samples were then treated with Lysonase™ (Millipore Sigma) for 30 min and clarified by centrifugation at 14,000g for 2 min at 4°C. Total protein concentrations were determined on microtiter plates using the Pierce™ BCA Protein Assay Kit (ThermoFisher Scientific) according to manufacturer's instructions and were used to normalize acetyl-P levels based on cell recovery. Remaining cell suspensions were extracted by addition of ¼ volume ice-cold 3M $HClO_4$ and incubated on ice for 30 minutes. After centrifugation, the supernatant was neutralized by addition of ¼ volume of saturated $KHCO_3$. The supernatant was incubated on ice with about 8 mg powdered activated charcoal per 100 µl lysate to remove any residual ATP/ADP for 15 min followed by a 0.22 µm Millex®-GV spin filtration (Millipore). Acetyl-Phosphate was converted to ATP by incubating 200 µl lysate with purified *E. coli* acetate kinase (Sigma Aldrich), ultrapure ADP (Cell technology) and $MgCl_2$ for 90min at 30°C. After incubation, aliquots of each sample were mixed with CellTiter-Glo® Luminescent Cell Viability (Promega) reagent in triplicates, and incubated for 10 min on a plate shaker. Luminescence was measured using a VICTOR3 plate reader (Perkin Elmer). The level of ATP contamination in samples

(background signal) was lower than 0.5% of total signal and the acetyl-phosphate conversion efficiency of the assay was estimated around 40% (control reactions).

Hydrogen peroxide sensitivity

Freshly transformed colonies of strains NM525 (WT), FDM1708 and FDM1750 were grown in LB medium supplemented with 100 µg/mL ampicillin and 1 mM IPTG for 5 hours (OD_{600} ~3-4, transition to stationary phase). Cells were then diluted to start with an OD_{600} of 0.05 in 1 ml of fresh LB medium (same concentration of ampicillin and IPTG) with or without 8 mM H_2O_2. The oxidative shock recovery was followed by measuring cell growth for 15 hours using the plate reader Tecan Spark® 20M. Strains unable to recover during this time-frame period were dead (unable to form colonies when plated).

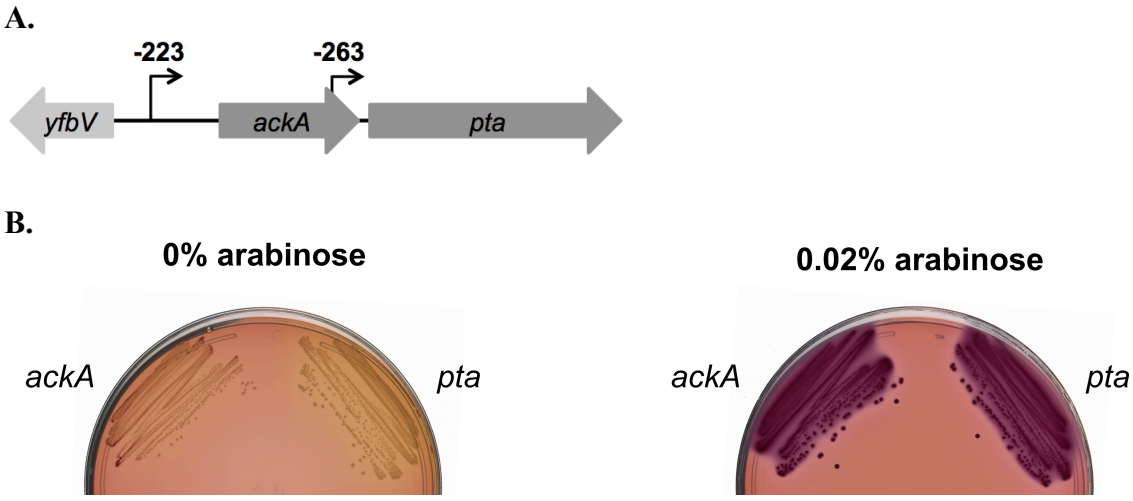

Fig. S1. Design of translational reporter fusions and determination of basal activities. Related to Fig. 2 and SI Appendix, Fig. S2.

A. Schematic representation of *ackA* and *pta* promoters. The *ackA-lacZ* and *pta-lacZ* translational fusions were constructed with a 5' leader of 223 and 263 nucleotides respectively, based on differential RNA sequencing data (3). Note that mapping in this paper of the *pta* promoter gives a start at -261.

B. Activity of P_{BAD}-*lacZ* translational fusions (*ackA*: FDM1700, *pta*: FDM1705) on MacConkey Lactose Agar. Reporter strains were streaked on MacConkey Lactose plates with or without arabinose to qualitatively determine the basal activity of each fusion. Plates were incubated at 37°C for 15 hours. The *ackA-lacZ* fusion was slightly active in the absence of arabinose (light pink colonies), suggesting the presence of a minor promoter within the *ackA* leader. This is consistent with a previous report of transcriptional activity between -42 and -143 in the leader sequence (12).

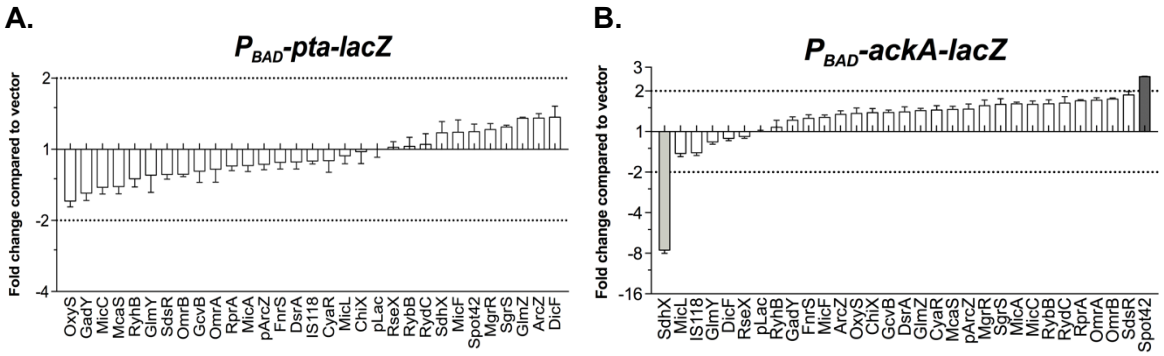

Fig. S2. Screening of the sRNA plasmid library in the *P_{BAD}-ackA-lacZ* and *P_{BAD}-pta-lacZ* translational reporter strains. Related to Figure 2.

A-D. Screening of the sRNA library with the *P_{BAD}-pta-lacZ* (FDM1705) (A) and *P_{BAD}-ackA-lacZ* (FDM1700) (B) translational fusions, in an otherwise WT background. Cells were grown in LB broth containing ampicillin (50μg/ml), IPTG (100μM) and arabinose concentrations chosen based on the activity of the fusion [0.002% (A); 0.02% (B)] in microtiter plates at 37°C for 6h and assayed as described in Materials and Methods. Light and dark grey bars indicate sRNAs having a significant repressing or an activating effect, respectively, on the fusion. Basal levels of expression of the fusions were 104 (A) and 80 (B) machine units, about 10x lower than Miller units.

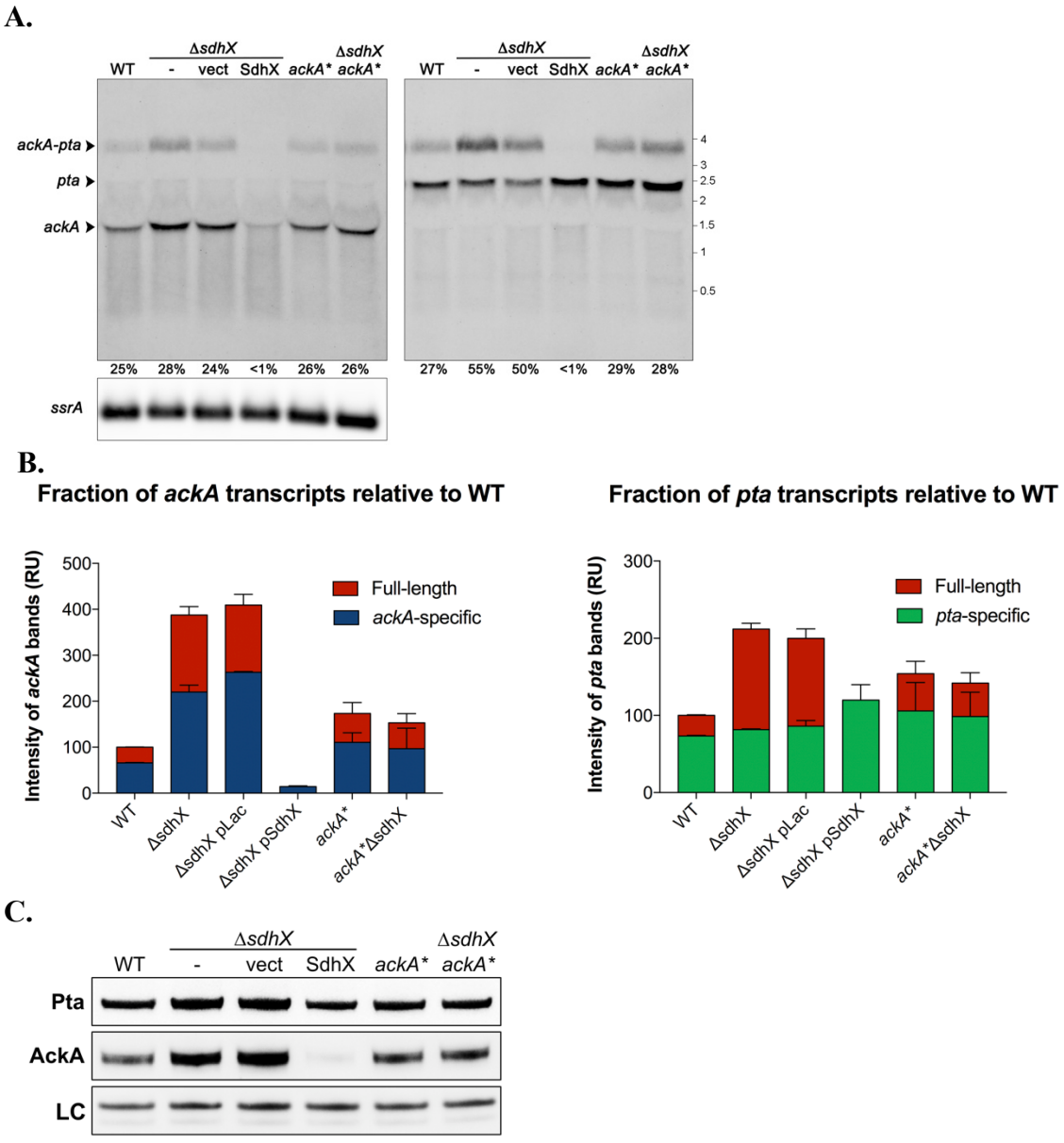

Fig. S3. SdhX enhances discoordinate expression of the *ackA-pta* operon. Related to Fig. 3.

A. Northern Blot analysis of *ackA* and *pta*. A wild type strain (NM525) and its derivatives Δ*sdhX* (FDM1708), *ackA** (FDM1712), and *ackA** Δ*sdhX* (FDM1713) were grown at 37°C in LB; in addition, Δ*sdhX* cells (FDM1708) carrying either the vector control or a plasmid encoding SdhX sRNA were grown in the presence of 100 μg/ml ampicillin and 100 μM IPTG to induce sRNA expression. Total RNA was extracted at OD_{600} of 1 and transcripts were probed independently for both *ackA* and *pta*. The numbers to the right give an estimation of band sizes in Kb. Numbers below the gels indicate the % of full-length transcript relative to the total *ackA* or *pta*-specific transcript, based on the band quantification of two independent experiments using ImageStudio software. SsrA serves as a loading control.

B. Relative intensity of *ackA*, *pta* and *ackA-pta* bands relative to WT cells, using the strains in SI Appendix, Fig. S3A. The quantification represents the mean ± SD of two independent experiments using ImageStudio software. Both *ackA* and *pta* mRNA were probed at the same time to amplify the weak individually-probed *ackA-pta* signal, improving quantification. Band intensities were normalized with SsrA as a loading control.
C. Western Blot of cells grown as in SI Appendix, Fig. S3A. Cells were collected at OD_{600} of 1 to analyze protein amounts of AckA and Pta-FLAG by Western Blot. Strains used to measure AckA and Pta-FLAG were derivatives of the strains listed in Fig. 3A, but carrying the FLAG-tagged *pta* gene (NM525: FDM1714; for FDM1708: FDM1715; for FDM1712:FDM1716 and for FDM1713:FDM1717. A stable non-specific band detected by the anti-AckA antibody serves as a loading control (LC).

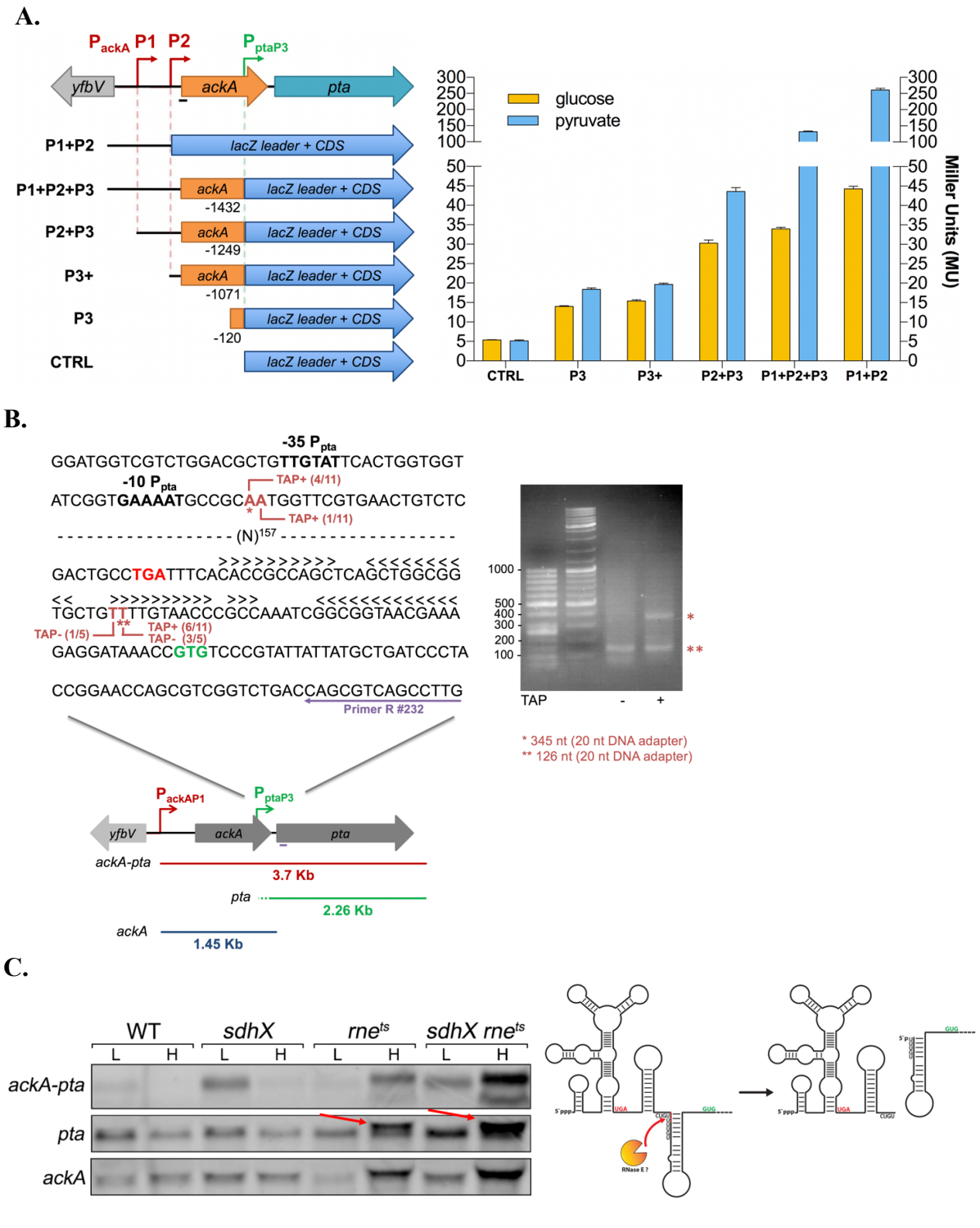

Fig. S4. An internal promoter inside the *ackA* CDS drives *pta* expression.

A. Activity of *pta-lacZ* transcriptional fusions reporter strains carrying different sequences upstream from the *pta* translation start codon, with promoters that are expected to be present (left panel; see SI Appendix, Table S1 for descriptions of specific strains). Cells were grown in MOPS minimal medium supplemented with glucose 0.2% (yellow bars) or sodium pyruvate 0.6% (blue

bars) until mid-exponential phase (OD_{600} of 0.4-0.5). Fusions labelled CTRL, P3, P3+, P2+P3, P1+P2+P3 and P1+P2 are respectively carried by FDM1719, FDM1720, FDM1721, FDM1722, FDM1723 and FDM1724. Error bars indicate SEM of three biological replicates.

B. Representation of 5′ RACE data covering the 3′ *ackA* CDS (241 nt) and the *ackA-pta* intergenic sequence (74 nt). The intergenic region is delimited by the red *ackA* stop codon (TGA) and the green *pta* start codon (GTG) and hairpin structures are indicated by arrow heads (> <). The putative upstream -10 and -35 promoter elements are annotated in bold. Cells (WT: NM525) were grown in LB and RNA extracted and treated as described in Supplemental Materials and Methods. TAP-treated and untreated PCR products were run on a 1% agarose gel before TOPO-cloning (right panel). The results are consistent with transcription initiation at the site marked with * (detected only after TAP treatment), and a processing site at the position marked with ** (detected both with and without TAP treatment).

C. Derivatives of NM525 carrying *rne*$^{+}$ or *rne*-3071 (temperature sensitive allele of RNase E essential endonuclease) were grown at 32°C (L) to an OD600 of 1, and then a portion of the culture was incubated at 43.5°C for 10 minutes (H) to inactivate the mutant RNase E. Samples were collected from both samples for Northern Blot analysis of *ackA* and *pta* transcripts. Strains used: WT: FDM1727; Δ*sdhX*: FDM1732; *rne-3071* (thermosensitive mutant): FDM1729; Δ*sdhX rne-3071*: FDM1731). Northern blot results suggest that RNase E is most likely responsible for the cleavage of the *ackA-pta* intergenic region, based on comparison of the *pta* transcript when the RNase E is active or not [compare WT to *rne* mutant at H (high temperature)]. Red arrows point to *pta* band that appears only when RNase E is inactivated. Schematic representation of the intergenic region processed by an endoribonuclease. The red TGA codon indicates the *ackA* stop codon and the green GTG indicates the *pta* start codon. Hairpin structures in the intergenic region are shown in SI Appendix, Fig. S4B by arrow heads. The processing should lead to *pta* transcripts carrying a 5′ monophosphate (5′P) followed by a hairpin.

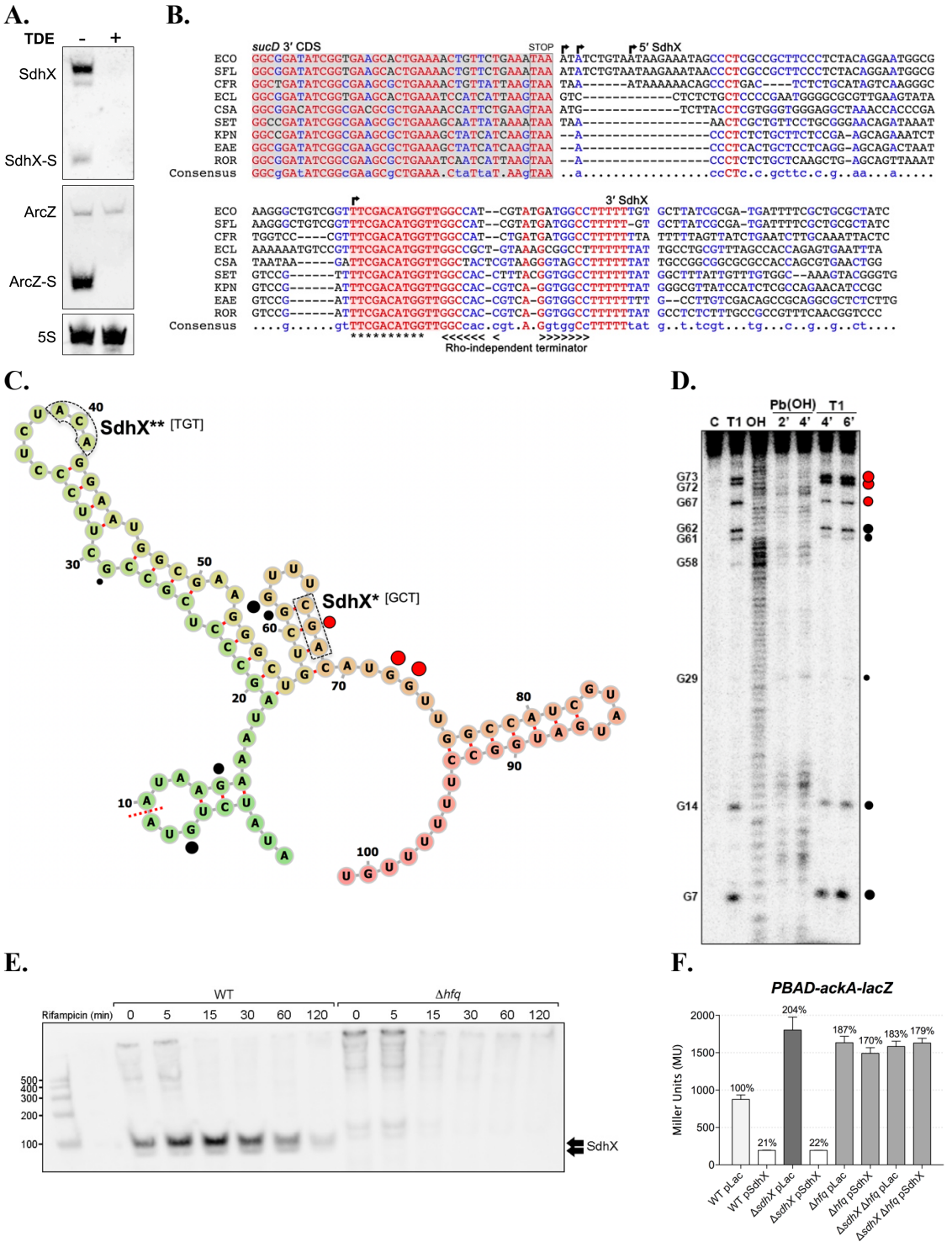

Fig. S5. SdhX is a processed and highly structured Hfq-dependent sRNA. Related to Fig. 4.

A. Terminator exonuclease analysis of SdhX. Total RNA isolated from MG1655 WT cells grown to OD_{600} ~2.5 in LB was left untreated (-) or incubated with 5′ monophosphate-dependent terminator exonuclease (TDE) (+) and analyzed as described in SI Appendix

Materials & Methods. The membrane was probed for SdhX (primer FDM41) and ArcZ (primer FDM42); ArcZ has been previously shown to be processed from a primary transcript (ArcZ) to an abundant shorter form (ArcZ-S). The two longer SdhX species defined by primer extension (Fig. 4B) constitute a broad non-resolvable band on the Northern Blot. The SdhX shorter form (SdhX-S) was not identified by primer extension (Fig. 4B); the primer (FDM17) used extended beyond the end of this form.

B. Sequence alignment of the *sucD* 3′ coding sequence (CDS, grey box) and 3′ UTR of related enterobacterial species. The arrows indicate the 5′ends of SdhX identified by 5′RACE in *Escherichia coli* (ECO); its conserved seed sequence is shaded in red. The seed region used to bind *ackA* mRNA is underscored with asterisks (*). Highly conserved nucleotides are annotated in red and partially conserved nucleotides are in blue. SFL: *Shigella flexneri*, CFR: *Citrobacter freundii*, ECL: *Enterobacter cloacae,* CSA: *Cronobacter sakazakii*, SET: *Salmonella enterica* Typhimurium, KPN: *Klebsiella pneumoniae*, EAE: *Enterobacter aerogenes*, ROR: *Raoultella ornithinolytica*.

C. Secondary structure of SdhX predicted by the RNAfold algorithm (13) and depicted by a color gradient representing the 5′ and 3′ ends of the sRNA, respectively in green and red. Sites of RNase T1 cleavage (SI Appendix, Fig. S5D) are indicated by solid black dots proportional to the amount of cleavage; cutting sites in the seed region (nts 64 to 75) are represented with solid red dots. The 5′ end of $SdhX_{92}$ is annotated by a dashed red line. Mutations of two SdhX variants used in the paper are highlighted with black dotted boxes.

D. *In vitro* structure probing of 5′ end-labeled SdhX sRNA by lead(II) acetate or RNase T1 cleavage. Lanes T1 and OH indicate RNase T1 or alkaline ladders of denaturated SdhX sRNA. The long GC-rich hairpin (nts 19 to 57) was not denatured under the denaturing conditions used here (see SI Appendix Materials and Methods). Sites of RNase T1 cleavage are indicated by solid dots proportional to the amount of cleavage.

E. Chase of SdhX transcripts with or without Hfq protein (WT: FDM1700, Δ*hfq*: FDM1725). Cells were grown to OD_{600} 1 in LB before extraction for Northern Blot analysis of SdhX. Samples were collected at the indicated times after addition of rifampicin. Data are representative of two independent experiments.

F. *ackA-lacZ* translational reporter variants (WT: FDM1700, Δ*sdhX*: FDM1701, Δ*hfq*: FDM1725, Δ*hfq* Δ*sdhX*: FDM1726) were transformed with the pBRpLac vector control or pSdhX plasmid, grown in flasks and assayed in stationary phase as for Fig. 2B. Three independent cultures were assayed for each strain and data are plotted as mean ± SD.

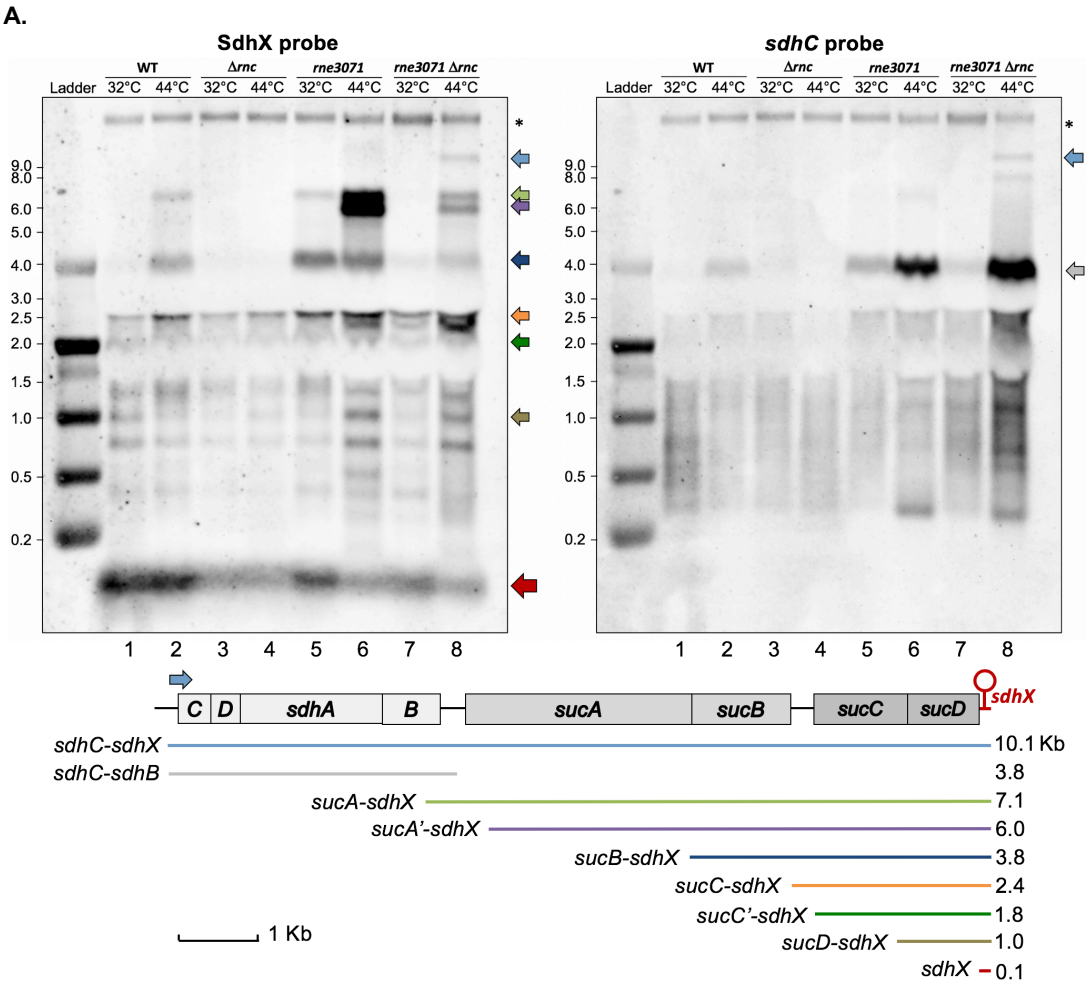
A.
SdhX probe
sdhC probe
WT
Δrnc
rne3071
rne3071 Δrnc
Ladder
32°C
44°C
9.0
8.0
6.0
5.0
4.0
3.0
2.5
2.0
1.5
1.0
0.5
0.2
*
1 2 3 4 5 6 7 8
C D sdhA B sucA sucB sucC sucD sdhX
sdhC-sdhX 10.1 Kb
sdhC-sdhB 3.8
sucA-sdhX 7.1
sucA'-sdhX 6.0
sucB-sdhX 3.8
sucC-sdhX 2.4
sucC'-sdhX 1.8
sucD-sdhX 1.0
sdhX 0.1
1 Kb

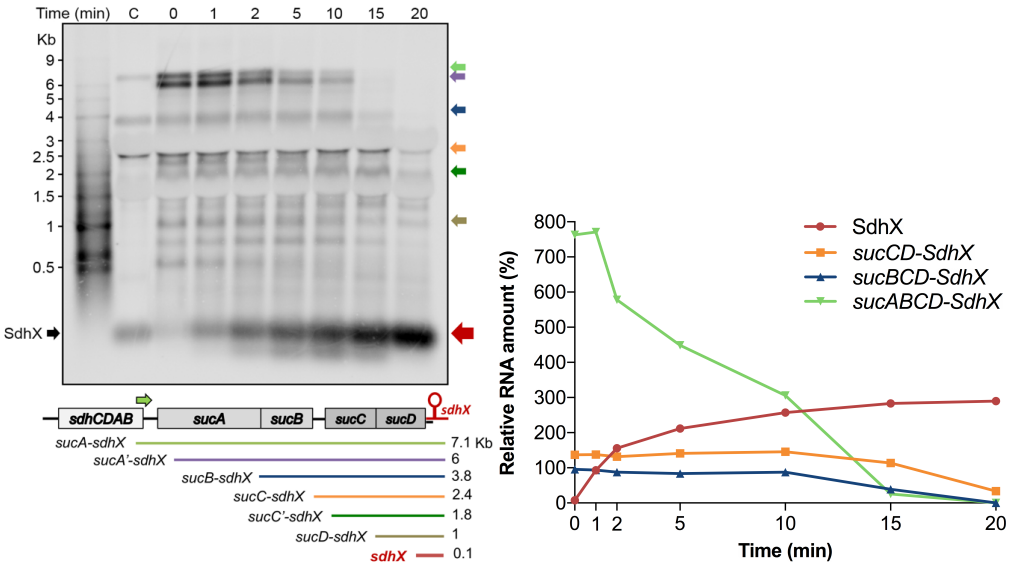
B.
Time (min) C 0 1 2 5 10 15 20
Kb
9
6
5
4
3
2.5
2
1.5
1
0.5
SdhX
sdhCDAB sucA sucB sucC sucD sdhX
sucA-sdhX 7.1 Kb
sucA'-sdhX 6
sucB-sdhX 3.8
sucC-sdhX 2.4
sucC'-sdhX 1.8
sucD-sdhX 1
sdhX 0.1
Relative RNA amount (%)
800
700
600
500
400
300
200
100
0
0 1 2 5 10 15 20
Time (min)
SdhX
sucCD-SdhX
sucBCD-SdhX
sucABCD-SdhX

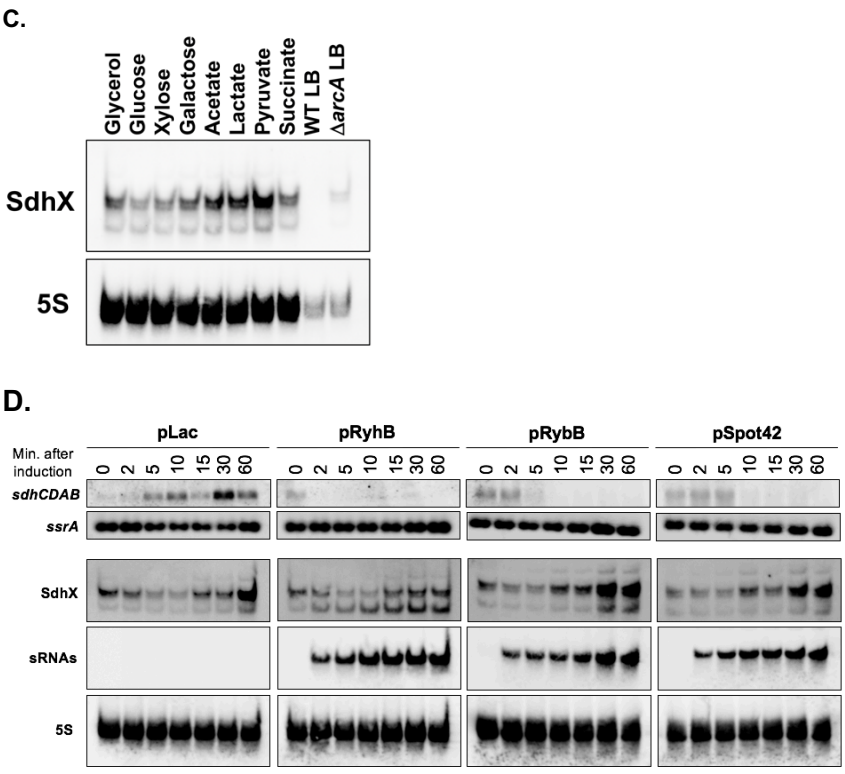

Fig. S6. SdhX biogenesis is dependent on the processing of *sdhCDAB-sucABCD* transcripts by RNase E but independent of the sRNA regulation of these transcripts. Related to Fig. 4.

A. Strains (*rnc* mutant: FDM1728, lanes 3-4; *rne-3071* thermosensitive mutant: FDM1729, lanes 5-6; *rnc rne-3071* double mutant: FDM1730, lanes 7-8; isogenic wild-type control: FDM1727, lanes 1-2) were grown at 32°C to an OD_{600} of ~2.5, then shifted to 43.5°C to inactivate RNase E. Samples were collected after 15 minutes, RNA extracted and analyzed as described in Materials and Methods, probing for SdhX (left panel) and *sdhC* (right panel). Each major band is labeled with a different color arrow corresponding to a specific processed transcript of the *sucABCD-sdhX* RNA, depicted below the gel and based on previous work (14), updated to include *sdhX*; the putative *sdhCDAB-sucABCD-sdhX* and *sucABCD-sdhX* primary transcripts are respectively shown in cyan (10.1 kB) and light green (7.1 kB). The top bands marked with an asterisk are non-specific and can be considered as a loading control.

B. Cleavage of SdhX from *sdhCDAB-sucABCD* mRNAs is dependent on RNase E. A *rne-3071* thermosensitive mutant (FDM1729) was grown at 32°C to OD_{600} of 1, then shifted to 43.5°C for 15 min to inactivate RNase E. Transcription was blocked by addition of rifampicin and cells were then immediately shifted back to 32°C. Total RNAs were extracted 0, 1, 2, 5, 10, 15 and 20 minutes after addition of rifampicin (chase), run on a gel and analyzed with the SdhX-specific biotinylated probe. The first lane (C) represents RNA extract from cells kept at 32°C, before the temperature shift. Major bands are labeled as for SI Appendix, Fig. S6A, except that the SdhX band is indicated with a red arrow. Note that the transcript for the full operon (10.1 kB band in Fig. 6A) is not seen here because RNase III is functional, cleaving between *sdhB* and *sucA*. Levels of *suc*-SdhX mRNA and SdhX sRNA are based on the Northern Blot quantification of the same blot using ImageStudio software.

C. Endogenous SdhX expression in MOPS minimal medium supplemented with different carbon sources as described in the Fig. 4 legend, or in LB medium with the Δ*arcA* derivative (FDM1733). Samples were collected in mid-exponential phase. Blots are representative of biological duplicates. See Fig. 4C for quantification of data.

D. Total RNAs were isolated from a Δ*spf* Δ*rybB* Δ*ryhB* strain (FDM1734) transformed with the indicated plasmids, and induced with 100μM IPTG (time=0) at OD_{600} of 1. Samples were collected at the indicated times after IPTG induction. Northern Blots were probed for *sdhC* mRNA and SdhX as well as the overexpressed sRNA. SsrA serves as a loading control for the mRNA gel. 5S rRNA serves as a loading control for the sRNA gel. Results are representative of two independent experiments.

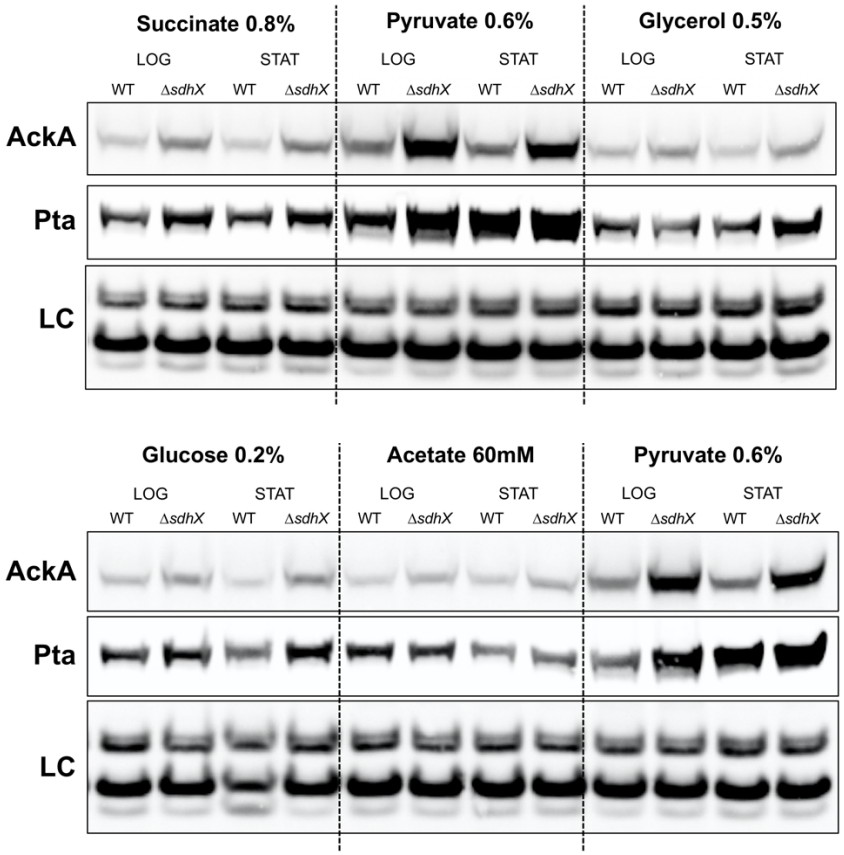

Fig. S7. Changes in AckA and Pta as a function of carbon source and SdhX. Related to Fig. 4D

WT (FDM1714) and Δ*sdhX* (FDM1715) cells were grown at 37°C in MOPS minimal medium supplemented with several carbon sources: 0.8% sodium succinate hexahydrate, 0.6% sodium pyruvate, 0.5% glycerol, 0.2% glucose and 60 mM sodium acetate. Samples were collected in exponential (OD_{600} of ~0.4) and stationary phases for each condition. Levels of the proteins were normalized to the level in pyruvate for the graph in Fig. 4D, allowing comparison between two separate experiments. LC serves as a loading control and represents non-specific bands detected by the anti-AckA antibody. Blots are representative of biological duplicates. See Fig. 4D for quantification of data.

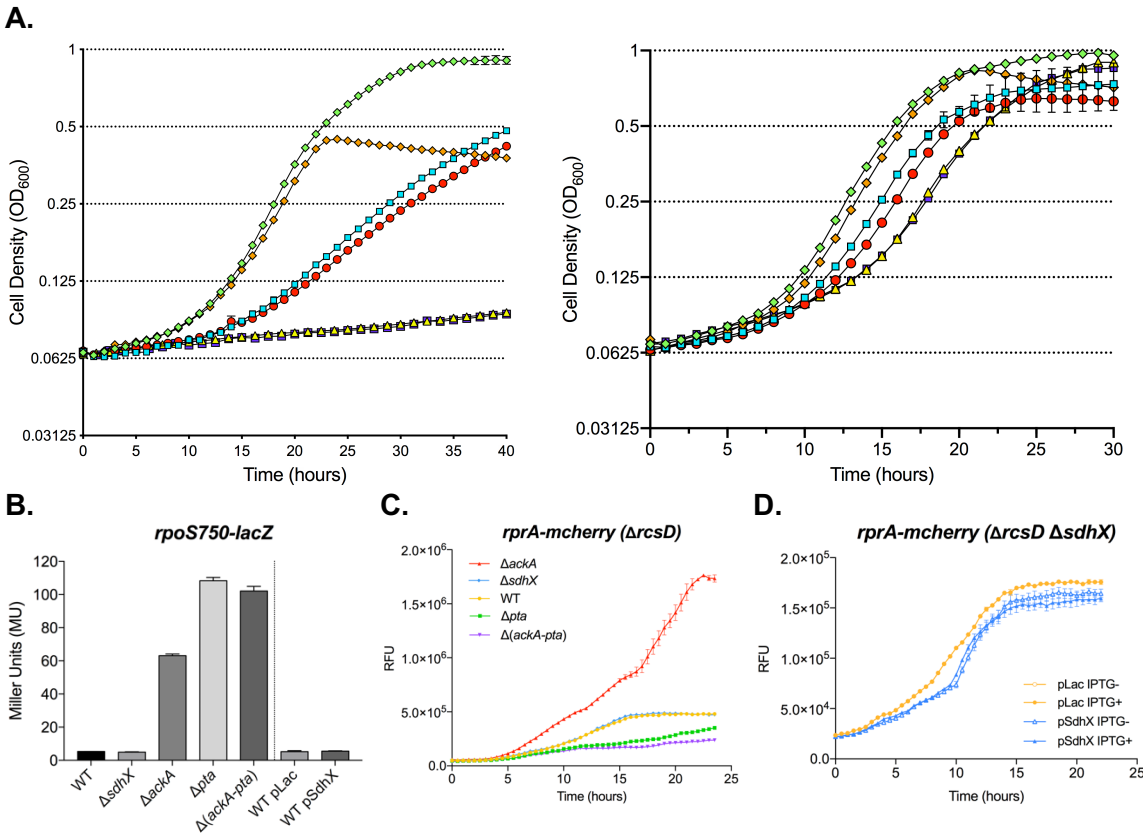

Fig. S8. SdhX-associated Phenotypes: Growth and Regulation. Related to Fig. 5.

A. Growth curve of SdhX^{seedless} (FDM1752, cyan squares), Δ*acs* (FDM1755, orange diamonds), Δ*acs* SdhX^{seedless} (FDM1756, red circles), Δ*ackA* (FDM1757, purple squares), Δ(*ackA-pta*) (FDM1758, yellow triangles) and its WT derivative (FDM1753, green diamonds) cells in MOPS minimal medium supplemented with 60 mM Na acetate (left panel) or 0.6% Na pyruvate (right panel). Growth curves of Δ*ackA* and Δ(*ackA-pta*) strains are overlapping in both conditions. Each curve represents the mean of two duplicates from colonies grown overnight in LB rich medium.

B. *rpoS750-lacZ* translational fusion reporter strains (WT: SG30013, Δ*sdhX*: FDM1735, Δ*ackA*: FDM1736, Δ*pta*: FDM1737, Δ(*ackA-pta*): FDM1738) were grown at OD_{600} of 1 in LB before assaying β-galactosidase activities (in Miller Units). Three independent cultures were assayed for each strain, data are plotted as mean ±SEM.

C. *rprA-mcherry* transcriptional fusion reporter variants (WT: EAW13, Δ*sdhX*: FDM1740, Δ*ackA*: FDM1741, Δ*pta*: FDM1742, Δ(*ackA-pta*): FDM1743) were grown in minimal medium supplemented with pyruvate 0.6% as carbon source. Relative Fluorescence Units were measured with Tecan Spark® 20M and adjusted to the growth rate (OD_{600}). Indicated RFU are plotted as mean ±SEM of 3 independent cultures.

D. *rprA-mcherry* transcriptional fusion reporter strain (Δ*sdhX*: FDM1740) transformed with pLac (orange circles) or pSdhX (blue triangles) were grown in minimal medium supplemented with pyruvate 0.6% as carbon source and 100 µg/ml ampicillin in the presence (filled shapes) or absence (empty shapes) of 100 µM IPTG. Relative Fluorescence

Units were measured with Tecan Spark® 20M and adjusted to the growth rate (OD_{600}). Indicated RFU are plotted as mean ±SEM of 3 independent cultures.

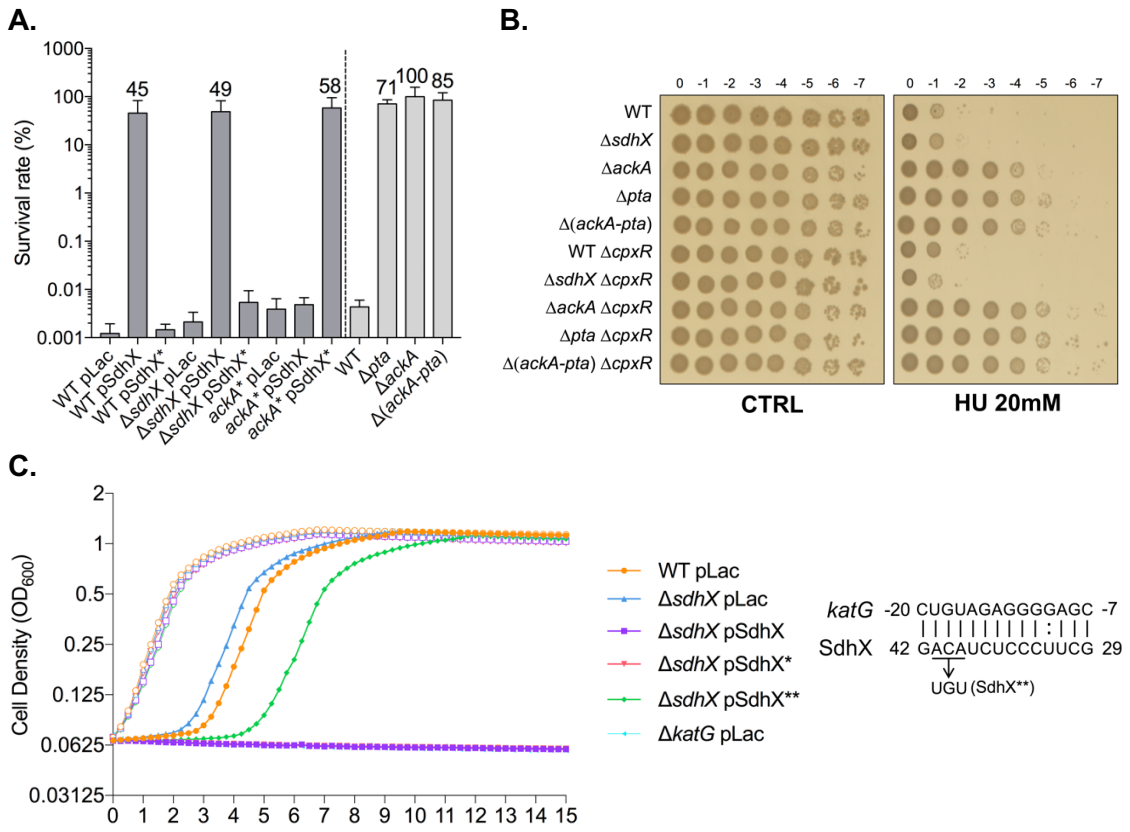

Fig. S9. SdhX-associated Phenotypes: Sensitivity to Stress Treatments. Related to Fig. 5.

A. Quantification of colony-forming units (CFUs) of cultures challenged with 20 mM hydroxyurea (HU) on LB plates or LB agar plates containing 20 mM hydroxyurea (HU), supplemented with ampicillin and IPTG 1 mM for left-hand panel (dark bars). Data (from experiments as shown in Fig. 5D) represent the mean of three independent experiments for each strain ±SD. Strains used were, for left hand panels (dark bars): WT (NM525), Δ*sdhX* (FDM1708) and *ackA** (FDM1712) transformed either with pLac, pSdhX or pSdhX* vectors; for right hand panel (lighter bars): WT (NM525), Δ*ackA* (FDM1709), Δ*pta* (FDM1711) and Δ(*ackA-pta*) (FDM1710).

B. Efficiency of plating spot assays on hydroxyurea as for Fig. 5D, and SI Appendix, Fig. S9A. Strains used: WT (NM525), Δ*sdhX* (FDM1708), Δ*ackA* (FDM1709), Δ*pta* (FDM1711), Δ(*ackA-pta*) (FDM1710) and Δ*cpxR* derivatives: respectively FDM1760, FDM1761, FDM1762, FDM1763, and FDM1764.

C. Growth curve of WT pLac, Δ*sdhX* pLac, Δ*sdhX* pSdhX, Δ*sdhX* pSdhX*, Δ*sdhX* pSdhX** and Δ*katG* pLac in LB medium supplemented with 8 mM of hydrogen peroxide (filled symbols). Untreated growth cultures (control) with 100 µg/ml ampicillin and 100 µM IPTG only are depicted with empty symbols. No growth was observed for Δ*sdhX* pSdhX, Δ*sdhX* pSdhX* or Δ*katG*. WT strain background is NM525, FDM1708 is the Δ*sdhX* derivative, FDM1750 is the Δ*katG* derivative. Data are representative of 3 independent experiments.

Table S1. Strains used in this study

Name	Genotype	Source
MG1655	*Wild type E. coli K-12* F- λ- *ilvG- rfb-50 rph-1*	Lab strain collection
PM1805	MG1655 *mal::lacI^{Q}*, Δ*araBAD araC^{+}*, *lacI′::P$_{BAD}$-cat-sacB-lacZ, mini-λ::tet*^{R}	(15)
NM1100	MG1655 *mini-λ::tet*^{R}	(16)
NM525	MG1655 *lacI^{Q} FLP-scar*	(3)
NM541	MG1655 *lacI^{Q} mini-λ::tet*^{R}	(17)
NM580	MG1655 *lacI^{Q}*, *ter1-ter2-zeo-P$_{lac}$-Kan-P$_{BAD}$-ccdB-lacZ*, *mini-λ::tet*^{R}	(17)
NM18	W3110 Δ*spf::cat*^{R}	(18)
PM1454	MG1655 *mal::lacI^{Q}*, Δ*araBAD araC^{+}*, *lacI′:: P$_{BAD}$-ryhA-lacZ*, Δ*arcA::kan*^{R}	Lab strain collection
KMT12055	DJ480 Δ*hfq::cat*^{R} *rybB-lacZ*	(19)
ASP6028	MG1655 Δ*tolC::kan*^{R}	(8)
GSO168	MG1655 Δ*rybB::kan*^{R}	(20)
EM1279	EM1055 *zce-726*::Tn*10*	(21)
EM1319	W3110 Δ*rnc::cat*^{R}	Lab strain collection
EM1277	EM1055 *rne-3071 zce-726*::Tn*10*	(21)
DJS2524	NM300 Δ*lac*X74 Δ*ryhB::kan*^{R}	(22)
FDM1700	MG1655 *mal::lacI^{Q}*, Δ*araBAD araC^{+}*, *lacI′:: P$_{BAD}$-ackA-lacZ*	This study[1]
FDM1701	MG1655 *mal::lacI^{Q}*, Δ*araBAD araC^{+}*, *lacI′:: P$_{BAD}$-ackA-lacZ*, Δ*sdhX::kan*^{R}	FDM1700 + P1 (FDM1608)
FDM1705	MG1655 *mal::lacI^{Q}*, Δ*araBAD araC^{+}*, *lacI′:: P$_{BAD}$-pta(-280)-lacZ*	This study[1]
FDM1706	MG1655 *mal::lacI^{Q}*, Δ*araBAD araC^{+}*, *lacI′:: P$_{BAD}$-ackA*-lacZ*	This study[1]
FDM1707	MG1655 *mal::lacI^{Q}*, Δ*araBAD araC^{+}*, *lacI′:: P$_{BAD}$-ackA*-lacZ*, Δ*sdhX::kan*^{R}	FDM1706 + P1 (FDM1708)
FDM1608	MG1655 Δ*sdhX::kan*$^{R\text{-}KEIO}$	NM1100 + PCR (FDM101-102)[2]
FDM1708	MG1655 *lacI^{Q} FLP-scar*, Δ*sdhX::kan*$^{R\text{-}KEIO}$	NM525 + P1 (FDM1608)
FDM1609	MG1655 Δ*ackA::kan*$^{R\text{-}KEIO}$	NM1100 + PCR (FDM103-104)[2]
FDM1709	MG1655 *lacI^{Q} FLP-scar*, Δ*ackA::kan*$^{R\text{-}KEIO}$	NM525 + P1 (FDM1609)
FDM1610	MG1655 Δ*ackA* Δ*pta::kan*$^{R\text{-}KEIO}$	NM1100 + PCR (FDM103-105)[2]
FDM1710	MG1655 *lacI^{Q} FLP-scar*, Δ(*ackA-pta*)*::kan*$^{R\text{-}KEIO}$	NM525 + P1 (FDM1610)
FDM1611	MG1655 Δ*pta::kan*$^{R\text{-}KEIO}$	NM1100 + PCR (FDM106-107)[2]
FDM1711	MG1655 *lacI^{Q} FLP-scar*, Δ*pta::kan*$^{R\text{-}KEIO}$	NM525 + P1 (FDM1611)
FDM1712	MG1655 *lacI^{Q} FLP-scar*, *ackA* T4A, C5G, G6C*	This study[1]
FDM1713	MG1655 *lacI^{Q} FLP-scar*, *ackA* T4A, C5G, G6C* Δ*sdhX::kan*$^{R\text{-}KEIO}$	FDM1712 + P1 (FDM1608)
FDM1614	MG1655 *lacI^{Q}*, *pta*-3×FLAG::*zeo*^{R}	This study[1]
FDM1714	MG1655 *lacI^{Q} FLP-scar*, *pta*-3×FLAG::*zeo*^{R}	NM525 + P1 (FDM1614)
FDM1715	MG1655 *lacI^{Q} FLP-scar*, Δ*sdhX::kan*$^{R\text{-}KEIO}$, *pta*-3×FLAG::*zeo*^{R}	FDM1708 + P1 (FDM1614)

FDM1716	MG1655 *lacI^{Q} FLP-scar*, *ackA* T4A C5G G6C, pta*-3×FLAG::*zeo*^{R}	This study[1]
FDM1717	MG1655 *lacI^{Q} FLP-scar*, *ackA* T4A C5G G6C, pta*-3×FLAG::*zeo*^{R}, Δ*sdhX::kan*$^{R\text{-}KEIO}$	FDM1716 + P1 (FDM1608)
FDM1719	MG1655 *lacI^{Q}*, *ter1-ter2-zeo- Ppta(-10)-lacZ*	This study[1]
FDM1720	MG1655 *lacI^{Q}*, *ter1-ter2-zeo-Ppta(-120)-lacZ*	This study[1]
FDM1721	MG1655 *lacI^{Q}*, *ter1-ter2-zeo-Ppta(-1071)-lacZ*	This study[1]
FDM1722	MG1655 *lacI^{Q}*, *ter1-ter2-zeo-Ppta(-1249)-lacZ*	This study[1]
FDM1723	MG1655 *lacI^{Q}*, *ter1-ter2-zeo-Ppta(-1432)-lacZ*	This study[1]
FDM1724	MG1655 *lacI^{Q}*, *ter1-ter2-zeo-PackAP2(-44)-lacZ*	This study[1]
FDM1725	MG1655 *mal::lacI^{Q}*, Δ*araBAD araC^{+}*, *lacI′::PBAD-ackA-lacZ*, Δ*hfq::cat*^{R}	FDM1700 +P1 (KMT12055)
FDM1726	MG1655 *mal::lacI^{Q}*, Δ*araBAD araC^{+}*, *lacI′::PBAD-ackA-lacZ*, Δ*hfq::cat*^{R}, Δ*sdhX::kan*$^{R\text{-}KEIO}$	FDM1725 + P1 (FDM1608)
FDM1727	MG1655 *lacI^{Q} FLP-scar*, *zce-726::Tn10*	NM525 + P1 (EM1279)
FDM1628	MG1655 *lacI^{Q} FLP-scar*, Δ*rnc::cat*^{R}	NM525 + P1 (EM1319)
FDM1728	MG1655 *lacI^{Q} FLP-scar*, *zce-726::Tn10*, Δ*rnc::cat*^{R}	FDM1628 + P1 (EM1279)
FDM1729	MG1655 *lacI^{Q} FLP-scar*, *rne-3071(Ts) zce-726::Tn10*	NM525 + P1 (EM1277)
FDM1730	MG1655 *lacI^{Q} FLP-scar*, *rne-3071(Ts) zce-726::Tn10*, Δ*rnc::cat*^{R}	FDM1628 + P1 (EM1277)
FDM1731	MG1655 *lacI^{Q} FLP-scar*, *rne-3071(Ts) zce-726::Tn10*, Δ*sdhX::kan*$^{R\text{-}KEIO}$	FDM1729 + P1 (FDM1608)
FDM1732	MG1655 *lacI^{Q} FLP-scar*, *zce-726::Tn10*, Δ*sdhX::kan*$^{R\text{-}KEIO}$	FDM1727 + P1 (FDM1608)
FDM1733	MG1655 *lacI^{Q} FLP-scar*, Δ*arcA::kan*^{R}	NM525 + P1 (PM1454)
FDM1632	MG1655 *lacI^{Q} FLP-scar*, Δ*spf::cat*^{R}	NM525 + P1 (NM18)
FDM1633	MG1655 *lacI^{Q} FLP-scar*, Δ*spf::cat*^{R}, Δ*rybB::kan*^{R}	FDM1632 + P1 (GSO168)
FDM1634	MG1655 *lacI^{Q} FLP-scar*, Δ*spf::cat*^{R}, Δ*rybB::FRT*	FDM1633 + FLP recomb.
FDM1734	MG1655 *lacI^{Q} FLP-scar*, Δ*spf::cat*^{R}, Δ*rybB::FRT*, Δ*ryhB::kan*^{R}	FDM1634 + P1 (DJS2524)
SG30013	DJ480 *rpoS750-lacZ*	(23)
FDM1735	DJ480 *rpoS750-lacZ*, Δ*sdhX::kan*$^{R\text{-}KEIO}$	SG30013 + P1 (FDM1608)
FDM1736	DJ480 *rpoS750-lacZ*, Δ*ackA::kan*$^{R\text{-}KEIO}$	SG30013 + P1 (FDM1609)
FDM1737	DJ480 *rpoS750-lacZ*, Δ*pta::kan*$^{R\text{-}KEIO}$	SG30013 + P1 (FDM1611)
FDM1738	DJ480 *rpoS750-lacZ*, Δ(*ackA-pta*)*::kan*$^{R\text{-}KEIO}$	SG30013 + P1 (FDM1610)
EAW13	NM857 *rprA-mcherry*, Δ*rcsD::FRT*	E. Wall (NCI)
FDM1740	NM857 *rprA-mcherry*, Δ*rcsD::FRT*, Δ*sdhX::kan*$^{R\text{-}KEIO}$	EAW13 + P1 (FDM1608)
FDM1741	NM857 *rprA-mcherry*, Δ*rcsD::FRT*, Δ*ackA::kan*$^{R\text{-}KEIO}$	EAW13 + P1 (FDM1609)
FDM1742	NM857 *rprA-mcherry*, Δ*rcsD::FRT*, Δ*pta::kan*$^{R\text{-}KEIO}$	EAW13 + P1 (FDM1611)
FDM1743	NM857 *rprA-mcherry*, Δ*rcsD::FRT*, Δ(*ackA-pta*)*::kan*$^{R\text{-}KEIO}$	EAW13 + P1 (FDM1610)
FDM1750	MG1655 *lacI^{Q} FLP-scar*, Δ*katG::kan*$^{R\text{-}KEIO}$	NM525 + P1 (KEIO)
FDM1652	MG1655 *lacI^{Q}*, SdhX^{seedless}-*zeo*^{R}	This study[1]
FDM1752	MG1655 *lacI^{Q} FLP-scar*, SdhX^{seedless}-*zeo*^{R}	NM525 + P1 (FDM1652)
FDM1653	MG1655 *lacI^{Q}*, SdhX^{+}-*zeo*^{R}	This study[1]

FDM1753	MG1655 *lacI^{Q} FLP-scar*, SdhX^{+}-*zeo*^{R}	NM525 + P1 (FDM1653)
FDM1654	MG1655, Δ*acs::kan*$^{R\text{-}KEIO}$	KEIO collection
FDM1754	MG1655 *lacI^{Q} FLP-scar*, Δ*acs::kan*$^{R\text{-}KEIO}$	NM525 + P1 (FDM1654)
FDM1755	MG1655 *lacI^{Q} FLP-scar*, SdhX^{+}-*zeo*^{R}, Δ*acs::kan*$^{R\text{-}KEIO}$	FDM1754 + P1 (FDM1653)
FDM1756	MG1655 *lacI^{Q} FLP-scar*, SdhX^{seedless}-*zeo*^{R}, Δ*acs::kan*$^{R\text{-}KEIO}$	FDM1754 + P1 (FDM1652)
FDM1757	MG1655 *lacI^{Q} FLP-scar*, SdhX^{+}-*zeo*^{R}, Δ*ackA::kan*$^{R\text{-}KEIO}$	FDM1709 + P1(FDM1653)
FDM1758	MG1655 *lacI^{Q} FLP-scar*, SdhX^{+}-*zeo*^{R}, Δ(*ackA-pta*)*::kan*$^{R\text{-}KEIO}$	FDM1710 + P1(FDM1653)
FDM1660	MG1655 *lacI^{Q}*, Δ*cpxR::zeo*^{R}	NM541 + PCR (FDM 35-36)[3]
FDM1760	MG1655 *lacI^{Q} FLP-scar*, Δ*cpxR::zeo*^{R}	NM525 + P1 (FDM1660)
FDM1761	MG1655 *lacI^{Q} FLP-scar*, Δ*sdhX::kan*$^{R\text{-}KEIO}$, Δ*cpxR::zeo*^{R}	FDM1708 + P1 (FDM1660)
FDM1762	MG1655 *lacI^{Q} FLP-scar*, Δ*ackA::kan*$^{R\text{-}KEIO}$, Δ*cpxR::zeo*^{R}	FDM1709 + P1 (FDM1660)
FDM1763	MG1655 *lacI^{Q} FLP-scar*, Δ*pta::kan*$^{R\text{-}KEIO}$, Δ*cpxR::zeo*^{R}	FDM1711 + P1 (FDM1660)
FDM1764	MG1655 *lacI^{Q} FLP-scar*, Δ(*ackA-pta*)*::kan*$^{R\text{-}KEIO}$, Δ*cpxR::zeo*^{R}	FDM1710 + P1 (FDM1660)

[1]See SI Appendix Material & Methods for details

[2]Strain ASP6028 was used as a template to amplify the kanamycin KEIO resistance cassette, designated here as *kan*$^{R\text{-}KEIO}$

[3]Strain NM580 was used as a template to amplify the zeocin resistance cassette (*zeo*^{R})

Table S2. Plasmids used in this study

Name	Genotype	Source
pBRpLac	*Parental plasmid containing Plac promoter, pBR322 origin, amp^R*	Lab plasmid collection[2]
pSdhX	*Wild type sdhX gene cloned into pBRplac AatII/EcoRI*	Lab plasmid collection[2]
pSdhX*	*mutant sdhX gene (C66G, G67C, A68T) from wild type pSdhX*	This study[1]
pSdhX**	*mutant sdhX gene (A39T, C40G, A41T) from wild type pSdhX*	This study[1]
pRyhB	*Wild type ryhB gene cloned into pBRplac AatII/EcoRI*	Lab plasmid collection[2]
pRybB	*Wild type rybB gene cloned into pBRplac AatII/EcoRI*	Lab plasmid collection[2]
pSpot42	*Wild type spf gene cloned into pBRplac AatII/EcoRI*	Lab plasmid collection[2]

[1]See SI Appendix Material & Methods for details
[2] Lab plasmid collection was constructed as described previously (1)

Table S3. Oligonucleotides, probes and synthetic gene fragments (gBlocks) used in this study

Primers	Genotype
FDM1	ACCTGACGCTTTTTATCGCAACTCTCTACTGTTTCTCCATCAGCCTGAAGGCCTAAGTAG
FDM2	TAACGCCAGGGTTTTCCCAGTCACGACGTTGTAAAACGACGTTCAGAACCAGTACTAACT
FDM3	TAACGCCAGGGTTTTCCCAGTCACGACGTTGTAAAACGACGTTCAGAACCAGTACTAACTTA CTGCTCATGGAAGTACCTATAATTGATACG
FDM4	ACCTGACGCTTTTTATCGCAACTCTCTACTGTTTCTCCATGTATCGGTGAAAATGCCGCA
FDM5	TAACGCCAGGGTTTTCCCAGTCACGACGTTGTAAAACGACAGGGATCAGCATAATAATAC
FDM12	GGGCTGTCGGTTTGCTCATGGTTGGCCATCGTATGATGG
FDM13	CCATCATACGATGGCCAACCATGAGCAAACCGACAGCCC
FDM14 gBlocks	CACCATCGCGCTGACTGCGATTCAGTCTGCACAGCAGCAGagcggatccgattataaagatcatgatggcgacta caaggaccacgatattgattacaaagacgatgacgataaataaTCTCGTCATCaaaaaggccatccgtcaggatggccttctttcaaaacagat aaaacgaaaggcccagtctttcgactgagcctttcgttttattTCTCTTAATTTGTTGACAATTAATCATCGGCATAGTA TATCGGCATAGTATAATACGACAAGGTGAGGAACTAAACCATGGCCAAGTTGACCAGTGCC GTTCCGGTGCTCACCGCGCGCGACGTCGCCGGAGCGGTCGAGTTCTGGACCGACCGGCTCG GGTTCTCCCGGGACTTCGTGGAGGACGACTTCGCCGGTGTGGTCCGGGACGACGTGACCCT GTTCATCAGCGCGGTCCAGGACCAGGTGGTGCCGGACAACACCCTGGCCTGGGTGTGGGTG CGCGGCCTGGACGAGCTGTACGCCGAGTGGTCGGAGGTCGTGTCCACGAACTTCCGGGACG CCTCCGGGCCGGCCATGACCGAGATCGGCGAGCAGCCGTGGGGGCGGGAGTTCGCCCTGCG CGACCCGGCCGGCAACTGCGTGCACTTCGTGGCCGAGGAGCAGGACTGAAGCTTTGCGCTG CGGATATCTGAACCGGAAATAATCACTA
FDM15	ACGTTTTTTTAGCCACGTATCAATTATAGGTACTTCCATGAGCAGTAAGTTAGTACTGGTTCT G
FDM16	CCTCTTTCGTTACCGCCGAT
FDM17	ACAAAAAAGGCCATCATACGATGGCCAACCATGTCGAAAC
FDM18	CCTGGCGGATATCGGTGAAGCAC
FDM20	TTGTCGTATTATACTATGCCGATATACTATGCCGATGATTAATTGTCAACGCAATGGTTCGTa ATTGTGAGCGGATAACAATTTCACACAGGAAACAGCTatgACCATGATTACGGATTCACTGGC CGTCGTTTTACAAC
FDM21	GTTGTAAAACGACGGCCAGTGAATCCGTAATCATGGTcatAGCTGTTTCCTGTGTGAAATTGT TATCCGCTCACAATtACGAACCATTGCGGCATTTTC
FDM22	ATACTATGCCGATATACTATGCCGATGATTAATTGTCAACGAAGCGCGCAATGGACGTTT
FDM23	ATACTATGCCGATATACTATGCCGATGATTAATTGTCAACACGCTCTATGGCTCCCTGAC
FDM24	ATACTATGCCGATATACTATGCCGATGATTAATTGTCAACTCCTTTAGCAGCCTGAAGGC
FDM25	ATACTATGCCGATATACTATGCCGATGATTAATTGTCAACGCGGCCACGTCTTTGAGTAATG
FDM26	GTTGTAAAACGACGGCCAGTGAATCCGTAATCATGGTcatAGCTGTTTCCTGTGTGAAATTGT TATCCGCTCACAATtCCATAGAGCGTAGCGCATGA
FDM27	GCCCTCGCCGCTTCCCTCTTGTGGAATGGCGAAGGGCTGTC
FDM28	GACAGCCCTTCGCCATTCCACAAGAGGGAAGCGGCGAGGGC
FDM30	rArCrUrCrUrCrUrArCrUrGrUrUrUrCrUrCrCrArU
FDM31	CAAGGCTGACGCTGGTCAGAC
FDM32	ACTCTCTACTGTTTCTCCAT
FDM35	AAGCAGAAACCATCAGATAGCCGCGACCACGCAAGGTTTTGTTGACAATTAATCATCGGC
FDM36	CGTAATTTCTGCCTCGGAGGTATTTAAACAatgAATAAAATCAGTCCTGCTCCTCGGCCA
FDM37	Biotin-CCGCAGTTCAGAACCAGTACTAACTTACTCG
FDM38	Biotin-GGCTGACGCTGGTCAGACCGACGCTGGTTC

FDM39	Biotin-CGCCACTAACAAACTAGCCTGATTAAGTTTTAACGC
FDM40	Biotin-GGCCATCATACGATGGCCAACCATGTCGAA
FDM41	Biotin-GAAACCGACAGCCCTTCGCCATTCCTGTAG
FDM42	Biotin-GGCTAGACCGGGGTGCGCGAATACTGCGCCAACACCAGGG
FDM43	Biotin-ATGGGGTCAGGTGGGACCACC
FDM44	Biotin-GAAACGCGATGGAGAATGGACGCTATCGCCGTGATG
FDM101	TGAAAACTGTTCTGAAATAAATATCTGTAATAAGAAATAGGATCCGTCGACCTGCAGTTC
FDM102	TCATCGCGATAAGCACAAAAAAGGCCATCATACGATGGCCGTGTAGGCTGGAGCTGCTTC
FDM103	TAGCCACGTATCAATTATAGGTACTTCCATGTCGAGTAAGGATCCGTCGACCTGCAGTTC
FDM104	CACCGCCAGCTGAGCTGGCGGTGTGAAATCAGGCAGTCAGGTGTAGGCTGGAGCTGCTTC
FDM105	CAGCGCAAAGCTGCGGATGATGACGAGATTACTGCTGCTGGTGTAGGCTGGAGCTGCTTC
FDM106	AACCCGCCAAATCGGCGGTAACGAAAGAGGATAAACCGTGGATCCGTCGACCTGCAGTTC
FDM107	AGATATCCGCAGCGCAAAGCTGCGGATGATGACGAGATTAGTGTAGGCTGGAGCTGCTTC
FDM108 gBlocks	CGTGAAAACCGTTCGCAGCCTGGCGGATATCGGTGAAGCACTGAAAACTGTTCTGAAATAA ATATCTGTAATAAGAAATAGCCCTCGCCGCTTCCCTCTACAGGAATGGCGAAGGGCTGTCG GGGCCATCGTATGATGGCCTTTTTTGTGCTCAGTCCTGCTCCTCGGCCACGAAGTGCACGCA GTTGCCGGCCGGGTCGCGCAGGGCGAACTCCCGCCCCCACGGCTGCTCGCCGATCTCGGTC ATGGCCGGCCCGGAGGCGTCCCGGAAGTTCGTGGACACGACCTCCGACCACTCGGCGTACA GCTCGTCCAGGCCGCGCACCCACACCCAGGCCAGGGTGTTGTCCGGCACCACCTGGTCCTG GACCGCGCTGATGAACAGGGTCACGTCGTCCCGGACCACACCGGCGAAGTCGTCCTCCACG AAGTCCCGGGAGAACCCGAGCCGGTCGGTCCAGAACTCGACCGCTCCGGCGACGTCGCGCG CGGTGAGCACCGGAACGGCACTGGTCAACTTGGCCATGGTTTAGTTCCTCACCTTGTCGTAT TATACTATGCCGATATACTATGCCGATGATTAATTGTCAACTTGCTTATCGCGATGATTTTCG CTGCGCTATCAGGGTAAATTT
FDM109 gBlocks	GTTTCGACATGGTTGGCCATCGTATGATGGCCTTTTTTGTGCTCAGTCCTGCTCCTCGGCCAC GAAGTGCACGCAGTTGCCGGCCGGGTCGCGCAGGGCGAACTCCCGCCCCCACGGCTGCTCG CCGATCTCGGTCATGGCCGGCCCGGAGGCGTCCCGGAAGTTCGTGGACACGACCTCCGACC ACTCGGCGTACAGCTCGTCCAGGCCGCGCACCCACACCCAGGCCAGGGTGTTGTCCGGCAC CACCTGGTCCTGGACCGCGCTGATGAACAGGGTCACGTCGTCCCGGACCACACCGGCGAAG TCGTCCTCCACGAAGTCCCGGGAGAACCCGAGCCGGTCGGTCCAGAACTCGACCGCTCCGG CGACGTCGCGCGCGGTGAGCACCGGAACGGCACTGGTCAACTTGGCCATGGTTTAGTTCCTC ACCTTGTCGTATTATACTATGCCGATATACTATGCCGATGATTAATTGTCAACTTGCTTATCG CGATGATTTTCGCTGCGCTATCAGGGTAAATTTA

Supplementary References

1. Mandin P, Gottesman S (2009) A genetic approach for finding small RNA regulators of genes of interest identifies RybC as regulating the DpiA/DpiB two-component system. *Mol. Microbiol.* 72:551-565.
2. Yu DG, et al. (2000) An efficient recombination system for chromosome engineering in *Escherichia coli*. *Proc. Natl. Acad. Sci. USA* 97:5978-5983.
3. Thomason MK, et al. (2015) Global transcriptional start site mapping using differential RNA sequencing reveals novel antisense RNAs in *Escherichia coli*. *J Bacteriol* 197:18-28.
4. Guillier M, Gottesman S (2006) Remodelling of the *Escherichia coli* outer membrane by two small regulatory RNAs. *Molec. Microbiol.* 59:231-247.
5. Miller JH (1972) *Experiments in Bacterial Genetics* (Cold Spring Harbor Laboratory Press, Cold Spring Harbor, New York) p 466.
6. Datsenko KA, Wanner BL (2000) One-step inactivation of chromosomal genes in *Escherichia coli* K-12 using PCR products. *Proc. Natl. Acad. Sci. USA* 97:6640-6645.
7. Baba T, et al. (2006) Construction of *Escherichia coli* K-12 in-frame, single-gene knockout mutants: the Keio collection. *Mol. Syst. Biol.* 2:2006.0008.
8. Parker A, Gottesman S (2016) Small RNA Regulation of TolC, the Outer Membrane Component of Bacterial Multidrug Transporters. *J Bacteriol* 198:1101-1113.
9. Cherepanov PP, Wackernagel W (1995) Gene disruption in *Escherichia coli*: TcR and KmR cassettes with the option of Flp-catalyzed excision of the antibiotic-resistance determinant. *Gene* 158:9-14.
10. Argaman L, et al. (2001) Novel small RNA-encoding genes in the intergenic region of *Escherichia coli*. *Curr. Biol.* 11:941-950.
11. Guo MS, et al. (2014) MicL, a new sigmaE-dependent sRNA, combats envelope stress by repressing synthesis of Lpp, the major outer membrane lipoprotein. *Genes Dev* 28:1620-1634.
12. Bakhtiari N, Mirshahi M, Babaeipour V, Maghsoudi N, Tahzibi A (2014) Down Regulation of ackA-pta Pathway in Escherichia coli BL21 (DE3): A Step Toward Optimized Recombinant Protein Expression System. *Jundishapur J Microbiol.* 7:1-9.
13. Mathews DH, et al. (2004) Incorporating chemical modification constraints into a dynamic programming algorithm for prediction of RNA secondary structure. *Proc Natl Acad Sci U S A* 101:7287-7292.
14. Cunningham L, Guest JR (1998) Transcription and transcript processing in the *sdhCDAB-sucABCD* operon of *Escherichia coli*. *Microbiology* 144 (Pt 8):2113-2123.
15. Lee HJ, Gottesman S (2016) sRNA roles in regulating transcriptional regulators: Lrp and SoxS regulation by sRNAs. *Nucleic Acids Res* 44:6907-6923.
16. Bougdour A, Cunning C, Baptiste PJ, Elliott T, Gottesman S (2008) Multiple pathways for regulation of σ^S (RpoS) stability in *Escherichia coli* via the action of multiple anti-adaptors. *Mol Microbiol* 68:298-313.
17. Battesti A, Majdalani N, Gottesman S (2015) Stress sigma factor RpoS degradation and translation are sensitive to the state of central metabolism. *Proc Natl Acad Sci U S A* 112:5159-5164.

18. Moon K, Gottesman S (2011) Competition among Hfq-binding small RNAs in *Escherichia coli*. *Molec. Microbiol.* 82:1545-1562.
19. Thompson KM, Rhodius VA, Gottesman S (2007) σ^E regulates and is regulated by a small RNA in *Escherichia coli*. *J. Bacteriol.* 189:4243-4256.
20. Hobbs EC, Astarita JL, Storz G (2010) Small RNAs and small proteins involved in resistance to cell envelope stress and acid shock in *Escherichia coli*: analysis of a bar-coded mutant collection. *J. Bacteriol.* 192:59-67.
21. Massé E, Escorcia FE, Gottesman S (2003) Coupled degradation of a small regulatory RNA and its mRNA targets in *Escherichia coli*. *Genes Dev* 17:2374-2383.
22. Santiago-Frangos A, Kavita K, Schu DJ, Gottesman S, Woodson SA (2016) C-terminal domain of the RNA chaperone Hfq drives sRNA competition and release of target RNA. *Proc Natl Acad Sci U S A* 113:E6089-E6096.
23. Zhou Y, Gottesman S (2006) Modes of regulation of RpoS by H-NS. *J. Bacteriol.* 188:7022-7025.